

<https://helda.helsinki.fi>

---

## Molecular Identification and Antifungal Properties of Four Thaumatococcal Proteins in Spruce (*Picea likiangensis*)

Liu, Yufeng

2021-09

---

Liu, Y., Liu, L., Asiegbo, F. O., Yang, C., Han, S., Yang, S., Zeng, Q. & Liu, Y. 2021, 'Molecular Identification and Antifungal Properties of Four Thaumatococcal Proteins in Spruce (*Picea likiangensis*)', *Forests*, vol. 12, no. 9, 1268. <https://doi.org/10.3390/f12091268>

---

<http://hdl.handle.net/10138/335025>

<https://doi.org/10.3390/f12091268>

---

cc\_by

publishedVersion

---

*Downloaded from Helda, University of Helsinki institutional repository.*

*This is an electronic reprint of the original article.*

*This reprint may differ from the original in pagination and typographic detail.*

*Please cite the original version.*

Article

# Molecular Identification and Antifungal Properties of Four Thaumatin-like Proteins in Spruce (*Picea likiangensis*)

Yufeng Liu <sup>1,2</sup> , Lijuan Liu <sup>1</sup>, Fred O. Asiegbu <sup>2</sup> , Chunlin Yang <sup>1</sup> , Shan Han <sup>1</sup>, Shuai Yang <sup>1</sup>, Qian Zeng <sup>1</sup> and Yinggao Liu <sup>1,\*</sup>

<sup>1</sup> College of Forestry, Sichuan Agricultural University, No. 211, Huimin Road, Wenjiang District, Chengdu 611130, China; liuyufeng6220245@163.com (Y.L.); liulijuan429@163.com (L.L.); yangcl0121@163.com (C.Y.); hanshan6618@163.com (S.H.); yangshuaiaihu@163.com (S.Y.); zq1573037145@163.com (Q.Z.)

<sup>2</sup> Department of Forest Sciences, University of Helsinki, Latokartanonkaari 7, FI-00014 Helsinki, Finland; fred.asiegbu@helsinki.fi

\* Correspondence: 11468@sicau.edu.cn

**Abstract:** Thaumatin-like proteins (TLPs) are involved in the plant defense response against pathogens, and most of them exhibit antifungal activity. However, the role of TLPs in pathogen-induced defense responses in spruce is not fully understood. In this study, four *TLP* genes encoding thaumatin-like protein, designated as *PITLP1–4*, were isolated and identified from *Picea likiangensis* needles. Sequence analysis showed that *PITLP1*, *PITLP3*, and *PITLP4* contained 16 conserved cysteine residues, while *PITLP2* had only 10 conserved cysteine residues. qPCR analysis showed that *PITLPs* were expressed in all tissues tested, *PITLP1*, *PITLP3*, and *PITLP4* had the highest expression levels in young fruits, while *PITLP2* had the highest expression levels in roots. In addition, the expression levels of four *PITLPs* were significantly upregulated during infection by *Lophodermium piceae*. Four recombinant *PITLPs* expressed in *Escherichia coli* exhibited obvious  $\beta$ -1,3-glucanase activity. The antifungal activity assay showed that four recombinant *PITLPs* had significant inhibitory effects on the mycelial growth of *L. piceae*, *Fusarium proliferatum*, *Botrytis cinerea*, and *Rousoella doimaesalongensis*. Microscopic observation revealed that the recombinant *PITLP1–4* induced the morphological changes of the mycelia of *L. piceae*, and the recombinant *PITLP2* and *PITLP3* induced the morphological changes of the mycelia of *F. proliferatum* and *R. doimaesalongensis*, while all the recombinant *PITLPs* had no obvious negative effect on the morphology of *B. cinerea* mycelium. These results suggest that *PITLP* genes may play an important role in the defense response of *P. likiangensis* against *L. piceae* invasion.

**Keywords:** *Picea likiangensis*; thaumatin-like protein; *Lophodermium piceae*;  $\beta$ -1,3-glucanase activity; antifungal activity



**Citation:** Liu, Y.; Liu, L.; Asiegbu, F.O.; Yang, C.; Han, S.; Yang, S.; Zeng, Q.; Liu, Y. Molecular Identification and Antifungal Properties of Four Thaumatin-like Proteins in Spruce (*Picea likiangensis*). *Forests* **2021**, *12*, 1268. <https://doi.org/10.3390/f12091268>

Academic Editors: Giovanni Emiliani and Alessio Giovannelli

Received: 1 June 2021

Accepted: 14 September 2021

Published: 17 September 2021

**Publisher's Note:** MDPI stays neutral with regard to jurisdictional claims in published maps and institutional affiliations.



**Copyright:** © 2021 by the authors. Licensee MDPI, Basel, Switzerland. This article is an open access article distributed under the terms and conditions of the Creative Commons Attribution (CC BY) license (<https://creativecommons.org/licenses/by/4.0/>).

## 1. Introduction

Forest trees are constantly faced with biotic and abiotic stresses throughout their life cycle, and have evolved a variety of mechanisms to protect themselves against these adverse environmental challenges [1]. Plants, including forest trees, possess constitutive and inducible defense mechanisms against attack from most pathogens, including physical and chemical barriers, synthesis of phytoalexins and expression of pathogenesis-related protein genes, etc. [2]. Pathogenesis-related (PR) proteins involved in host defense are induced when plants are infected by pathogenic fungi or bacteria and play an important role in plant adaptation to biotic and abiotic stresses [3,4]. PR proteins are generally classified into 17 different families based on their physicochemical properties and biological functions, and most of them have antifungal activity [5,6]. In addition, two putative novel families (PR18 and PR19) have been recently proposed [7]. Thaumatin-like proteins (TLPs), as the members of the PR5 protein family, are named because their amino acid sequences

are highly similar to that of the thaumatin isolated from the fruit of West African shrub *Thaumatococcus danielli* [8]. However, the functions of these two proteins are completely different. Thaumatinins have a sweet taste but no antifungal activity, while TLPs have the opposite properties [9]. Most TLP proteins contain a thaumatin signature (G-x-[GF]-x-C-x-T-[GA]-D-C-x(1,2)-[GQ]-x(2,3)-C) with a molecular mass in the range of 21–26 kDa, and 16 cysteine residues that form eight disulfide bonds. A small number of TLP proteins have a molecular weight of approximately 16–17 kDa and only contain 10 conserved cysteine residues that form five disulfide bonds [10,11]. These disulfide bonds not only contribute to maintaining the stability of the protein structure, but also strengthening the resistance of TLP proteins to protease degradation, extreme temperature, and pH conditions [12,13].

At present, TLP genes have been identified from a variety of plants [6,14–16], but only a few in conifers. The expression of TLP genes can be induced by a variety of factors, such as salicylic acid, methyl jasmonate, abscisic acid, wounding, UV, osmotic stress, and the invasion of pathogens such as bacteria, fungi, and viruses [17,18]. Many studies have shown that plant TLP genes play an important role in plant resistance to biotic stress, especially to infection by pathogenic fungi [19,20]. It has been reported that the constitutive expression of *GbTLP1* from *Gossypium barbadense* in transgenic tobacco plants exhibits considerable resistance against *Verticillium dahliae* and *F. oxysporum* [21]. TLP genes are also widely involved in the defense mechanism of tree species against pathogens. For example, expression of the TLP gene in *Pinus sylvestris* was up-regulated after inoculation with pathogenic fungi *Heterobasidion annosum* [17]. The expression levels of multiple *PmTLP* genes in *Pinus monticola* seedlings were up-regulated after being infected by blister rust pathogen *Cronartium ribicola* [22]. Over-expression of the *PeTLP* gene in transgenic poplars showed enhanced resistance against *Marssonina brunnea* [23]. In addition, some TLP genes have also been reported to confer tolerance to abiotic stresses such as drought, salt, and low temperatures in transgenic plants [17,21,24,25].

Currently, the use of environmentally harmful chemical pesticides in plant disease control is forbidden, and environmentally friendly biological control is urgently needed to be developed. Most of the TLP proteins reported have antifungal activity under in vitro conditions, so they have potential application value in the biological control of plant pathogens. A previous report showed that recombinant TLP from wheat was confirmed to have inhibitory activity against *Saccharomyces cerevisiae* [26]. A *Panax notoginseng* recombinant PnTLP2 expressed in *Escherichia coli* has antifungal effects in *Alternaria panax* and *Alternaria alternata* [11]. Moreover, a *PeTLP* gene from hybrid poplar was expressed by *E. coli*, and the recombinant PeTLP protein exhibited inhibitory activity against mycelial growth of three fungal species [27]. The antifungal mechanism of TLP proteins has also attracted the attention of scientists. Previous reports revealed that the antifungal properties of TLP proteins may be related to their ability to bind glucan or glucanase activity [18,28,29]. TLP proteins can bind and degrade  $\beta$ -1,3-glucan, which is the main component of the fungal cell wall [30], laying the foundation for TLP proteins to further damage the fungal cell membrane [31]. For instance, a rice TLP protein with glucanase activity showed a significant inhibitory effect on the growth of *Sclerotinia sclerotiorum* and could change the permeability of the hyphal membrane [32]. Furthermore, many TLP proteins with antifungal activity can penetrate the fungal cell membrane and increase the content of reactive oxygen species (ROS) in the cell, leading to oxidative damage [18,33].

*Picea likiangensis* is one of the dominant tree species in the subalpine forest of southwest China. Because of its wide distribution and large quantity, it plays an important ecological role in soil and water conservation and carbon accumulation in the subalpine region of southwest China. *Lophodermium* species are considered to be common foliar endophytes, saprotrophs, and pathogens of conifer trees [34]. In European coniferous forests, *Lophodermium piceae* is a major endophytic fungus in the needles of Norway spruce and plays an important role in needle decay [35]. However, *L. piceae* is considered to be the main pathogen of spruce needle cast disease in spruce plantations in southwest China, which causes a large number of spruce needles to drop, and further leads to low growth

and even death of spruce trees [36]. To our knowledge, there are no reports on *TLP* genes and their roles in spruce defense against needle disease. Considering the importance of *TLP* genes in plant disease resistance and antifungal activity, it is necessary to explore their role in *P. likiangensis* against *L. piceae*. In this study, we report the identification of four *TLP* genes from *P. likiangensis*. The expression profiles of *PITLP* genes in different tissues of *P. likiangensis* and during *L. piceae* invasion were analyzed by qPCR. In addition, the *PITLP* genes were expressed in *E. coli*, and the  $\beta$ -1,3-glucanase activity of the obtained recombinant proteins was evaluated. Furthermore, the antifungal activity of the recombinant proteins against four phytopathogenic fungi including *L. piceae* was determined. The objective of this study is to provide useful information for future research on the interaction between *P. likiangensis* and *L. piceae* invasion and lay the foundations for further exploring the function of *PITLP* genes.

## 2. Materials and Methods

### 2.1. Plant Materials, Plasmids and Strains

In this study, 20-year-old *Picea likiangensis* trees from a forest farm (N:29.51.15.78; E:102.15.34.49) in Luding County, Sichuan province, China, were used as the plant material. These trees were grown in natural conditions (altitude: 2721.00 m; precipitation/annual average: 625.18 mm; temperature/annual average: 10 °C). The roots, phloem (inner bark), twigs, needles, and young fruits were sampled from three healthy *P. likiangensis* trees for gene tissue expression analysis. The needles without *L. piceae* infection were regarded as the control group, while the needles sampled from three *P. likiangensis* trees naturally infected by *L. piceae* were treated as the test group. All samples were immediately frozen in liquid nitrogen and stored at −80 °C until further RNA extraction.

The pMD19-T vector used for gene cloning was purchased from TaKaRa (TaKaRa, Ōtsu, Japan). The pET-32a plasmid used for protein expression was provided by our lab (the Key Laboratory of National Forestry and Grassland Administration on Forest Resources Conservation and Ecological Safety in the Upper Reaches of the Yangtze River, College of Forestry, Sichuan Agricultural University, Chengdu, Sichuan, China). *Escherichia coli* (*E. coli*) Trans5 $\alpha$  chemically competent cells used for gene cloning and *E. coli* BL21(DE3) chemically competent cells used for prokaryotic expression were purchased from TransGen Biotech Co., Ltd. (Beijing, China).

### 2.2. Total RNA Extraction and cDNA Synthesis

Total RNA from each sample was extracted and treated with RNase-free DNase I using a Quick RNA Isolation Kit (Huayueyang, Beijing, China) according to the manufacturer's instructions. The integrity and concentration of total RNA were analyzed by using 1% agarose gel and the spectrophotometer (BioMate 3S, Thermo, Waltham, MA, USA), respectively. Approximately 2  $\mu$ g of total RNA was used for cDNA synthesis and was carried out by using PrimeScript<sup>TM</sup> RT Reagent Kit (TaKaRa, Ōtsu, Japan) under the manufacturer's instructions. The cDNA was stored at −20 °C for subsequent analysis.

### 2.3. PCR Amplification

Full-length sequences of four *PITLP* genes were obtained from our transcriptome library (unpublished) in *P. likiangensis*. The specific primers used for PCR amplification were designed using Primer Premier 5.0 tool (Table S1). The PCR reaction was performed on an A200 thermal cycler (LongGene, Hangzhou, China). The reaction mixture consisted of 1  $\mu$ L of *P. likiangensis* cDNA, 1  $\mu$ L of (10  $\mu$ M) forward/reverse primers, 12.5  $\mu$ L of 2 $\times$ TransTaq<sup>®</sup> High Fidelity (HiFi) PCR SuperMix II (-dye) (TransGen, Beijing, China), 9.5  $\mu$ L of ddH<sub>2</sub>O, in a total volume of 25  $\mu$ L. The amplification procedure was performed at 95 °C for 4 min, followed by 40 cycles, each of 95 °C for 40 s, 55 °C for 40 s, and 72 °C for 1 min 30 s; and a final extension at 72 °C for 10 min. The amplified product was detected by 1% (M/V) agarose gel electrophoresis and purified using a DNA Purification Kit (Solarbio, Beijing, China). The purified PCR product was ligated into the pMD19-T vector and then

transformed into *E. coli* Trans5 $\alpha$  cells. The transformed cells were screened by 100  $\mu$ g/mL ampicillin and identified by the above PCR conditions. Positive recombinant clones were sequenced at TSINGKE (TSINGKE, Chengdu, China).

#### 2.4. Sequence Analysis

The full-length cDNA sequence and deduced amino acid sequence of these genes were analyzed using DNAMAN 6.0 program (Lynnon Biosoft, Quebec City, QC, Canada). The molecular mass and theoretical isoelectric point (pI) were predicted using the ProtParam tool (<https://web.expasy.org/protparam/>, accessed on 10 March 2021). Prediction of a signal peptide was performed using SignalP (<http://www.cbs.dtu.dk/services/SignalP/>, accessed on 10 March 2021). The subcellular localization of the protein was evaluated using the PSORT tool (<https://www.genscript.com/psort.html>, accessed on 10 March 2021). The functional sites and domains of the protein sequence were analyzed on PROSITE (<https://prosite.expasy.org/>, accessed on 11 March 2021) and BLAST (<https://blast.ncbi.nlm.nih.gov/Blast.cgi>, accessed on 11 March 2021). Multiple sequence alignments were performed using the ClustalW program (<http://www.ebi.ac.uk/clustalw/>, accessed on 11 March 2021). The phylogenetic analysis was carried out using the neighbor-joining method with 1000 bootstrap replicates in the MEGA 6.0 program [37]. The tertiary structure of the protein was constructed using the SWISS-MODEL server (<https://swissmodel.expasy.org/>, accessed on 12 March 2021).

#### 2.5. qPCR Analysis

Specific primers for gene expression analysis were designed based on the CDS sequences of the four genes (Table S1). Elongation factor-1  $\alpha$  (EF1- $\alpha$ ) gene and translation initiation factor 5A (TIF5A) gene (GenBank accession number AJ132534.1 and DR448953, respectively) were used as two endogenous controls, and their primers are shown in Table S1. The qPCR reaction was performed using TB Green<sup>®</sup> Premix Ex Taq<sup>™</sup> II (Tli RNaseH Plus) (TaKaRa, Ōtsu, Japan) according to the manufacturer's instructions. Each reaction mixture consisted of 12.5  $\mu$ L of TB Green Premix Ex Taq II, 2  $\mu$ L of cDNA, 1  $\mu$ L of (10  $\mu$ M) forward/reverse primers, and 8.5  $\mu$ L of sterile H<sub>2</sub>O, with a total volume of 25  $\mu$ L. The thermal cycle parameters were as follows: 95 °C for 30 s, 40 cycles at 95 °C for 5 s and 60 °C for 30 s, and then a melt-curve analysis was performed with a constant increase from 65 °C to 95 °C. qPCR analysis was carried out with three technical replicates. The relative gene expression levels were calculated by the  $2^{-\Delta\Delta C_t}$  method [38]. Significance analysis of the data was performed using SPSS version 27.0 (SPSS Inc., Chicago, IL, USA).

#### 2.6. Recombinant Protein Expression

The mature peptide sequences of the four genes were amplified by PCR with specific primers containing *Eco*R I and *Xho* I restriction enzyme sites (Table S1). The amplified product was subcloned into the pET-32a vector, and the positive recombinant plasmid identified by PCR and sequencing was inserted into *E. coli* BL21 (DE3) chemically competent cells by heat shock for 45 s at 42 °C. Transformed cells were cultured in Luria-Bertani (LB) liquid medium containing 100  $\mu$ g/mL ampicillin at 37 °C with shaking for 12 h, and then the cultured cells were transferred to LB liquid medium (100  $\mu$ g/mL ampicillin) at a volume ratio of (1:100) and cultured at 37 °C until optical density 600 = 0.8. To maximize recombinant protein production, the induced expression conditions of isopropyl- $\beta$ -D-1-thiogalactopyranoside (IPTG) concentration and temperature were optimized. IPTG (final concentrations of 0, 0.2, 0.4, 0.6, 0.8, and 1.0 mM) were added to the cell medium at 37 °C for 3 h, respectively. In addition, the cells were induced with 0.2 mM IPTG at different temperatures (17 °C, 27 °C and 37 °C) for 3 h, respectively. The cells were collected by centrifugation at 10,000 g for 10 min and resuspended in sterile ddH<sub>2</sub>O. To evaluate the solubility distribution of the recombinant protein induced by different temperatures, the resuspended cells were frozen in liquid nitrogen and thawed in a 42 °C water bath, repeated six times. The supernatant and sediment of the disrupted cells were



collected separately by centrifugation at 4 °C for 30 min. The supernatant was further purified using His-tag Protein Purification Kit (Beyotime, Shanghai, China) according to the manufacturer's instructions. The recombinant protein was detected by 12% SDS-PAGE gel. The concentration of purified protein was determined according to the method of Liu et al. [36].

### 2.7. Enzyme Properties of Recombinant Protein

To explore whether the recombinant protein has  $\beta$ -1,3-glucanase activity. The enzyme activity of the recombinant protein was determined by measuring the hydrolysis of laminarin as a substrate. The reaction mixture containing 1% laminarin and 1 nmol of (0.2 mg/mL) recombinant protein was incubated in 50 mM sodium acetate buffer (pH 6.0) for 30 min at 40 °C. Subsequently, 2 mL of 3,5-dinitrosalicylic acid (DNS) solution was added at 100 °C for 10 min and finally placed on ice for 2 min to terminate the reaction. The released amount of reducing sugar was measured using a spectrophotometer (UV-1800PC, Mapada, Shanghai, China) at 520 nm. One unit (U) of enzyme activity was defined as the amount of enzyme that released 1  $\mu$ mol of glucose per minute under the above-measured conditions.

To evaluate the optimal pH of the enzyme activity of the recombinant protein, the enzyme activity of the recombinant protein was measured in two buffers (50 mM) with different pH: sodium acetate (pH 3, 4, 5, and 6) and Tris-HCl (pH 7, 8, and 9). The effect of temperature on the enzyme activity of the recombinant protein was measured at different temperatures (30, 40, 50, 60, 70 and 80 °C) in 50 mM sodium acetate buffer (pH6.0). The enzyme activity assay was completed with three replicates.

### 2.8. Antifungal Activity of Recombinant Protein

The antifungal activity of the four recombinant proteins was tested on four plant pathogenic fungi collected from our lab. The fungi tested included: *L. piceae*, *Fusarium proliferatum*, *Botrytis cinerea*, and *Roussioella doimaesalongensis*. These fungal strains were inoculated separately on potato dextrose agar (PDA) medium until the entire plate was covered. A 5 mm (diameter) fungal disk was inoculated into PDA medium containing 1 nmol of (0.2 mg/mL) recombinant protein. *L. piceae* was cultured on the plate containing the recombinant protein at 25 °C for 15 d, while *F. proliferatum*, *B. cinerea*, and *R. doimaesalongensis* were cultured on the plate containing the recombinant protein at 25 °C for 5 d, respectively. As a control, a 5 mm (diameter) fungal disk was inoculated on PDA medium without the recombinant protein. The results were presented as a percentage of relative growth in the control. To further observe the effect of the recombinant protein on the morphology of mycelia, we soaked a few mycelia into 1 nmol of (0.2 mg/mL) recombinant protein solution and treated them at 25 °C for 48 h. Sterile water was utilized as a control. The morphology of mycelium was observed by an electron microscope (Olympus BX43, Tokyo, Japan). Each fungal species was performed in three independent replicates. The significant inhibition of the recombinant protein on mycelial growth was assessed by SPSS version 27.0 (SPSS Inc., Chicago, IL, USA).

## 3. Results

### 3.1. Identification and Sequence Analysis of PITLPs

In this study, the full-length cDNA sequences of four PITLP genes from *P. likiangensis* were cloned based on the transcriptome library of *P. likiangensis*. The coding sequences (CDS) of PITLP1–PITLP4 were 705–969 bp in length and encoded 234–322 amino acid residues (Table 1). ProtParam analysis showed that the calculated molecular weights (MW) of the four deduced PITLP proteins were 24.684–33.450 kDa, and their theoretical isoelectric points (pI) ranged from 4.57 to 8.83 (Table 1). The full-length cDNA sequences of the four PITLP genes were deposited in GenBank, and the accession numbers were MW605094–MW605097.

**Table 1.** Characteristics of *P. likiangensis* PITLP genes.

Gene Name	CDS Length (bp)	Amino Acids No.	MW (kDa)	pI
<i>PITLP1</i>	705	234	24.869	8.83
<i>PITLP2</i>	747	248	26.775	8.52
<i>PITLP3</i>	705	234	24.684	4.57
<i>PITLP4</i>	969	322	33.450	4.86

BLAST analysis suggested that PITLP proteins were highly homologous to TLPs from other plant species. Specifically, *PITLP1* shared 88.03% sequence identity with PmTLP2 from *P. monticola*, and *PITLP3* shared 90.60% sequence identity with PsTLP from *P. sylvestris*. SignalP analysis showed that *PITLP1*, *PITLP2*, *PITLP3*, and *PITLP4* have an N-terminal signal peptide sequence of 31, 31, 30, and 20 amino acid residues, respectively (Figures S1–S4). PSORT predictions indicated that the four PITLP proteins were located in the extracellular region (Table 1). BLAST and PROSITE revealed that *PITLP1*, *PITLP3*, and *PITLP4* have a thaumatin family signature (G-x-[GF]-x-C-x-T-[GA]-D-C-x(1,2)-[GQ]-x(2,3)-C) (Figures S1, S3 and S4) [11]. Interestingly, although the *PITLP2* has a conserved domain of the thaumatin family, the typical signature sequence of the thaumatin family was not detected. Further analysis by PROSITE showed that *PITLP1*, *PITLP3*, and *PITLP4* contain 16 cysteine residues, which can form eight disulfide bonds. However, *PITLP2* has only five disulfide bonds formed by 10 cysteine residues (Figure 1).

A phylogenetic tree was constructed by MEGA6.0 to clarify the evolutionary relationship between the four PITLP proteins from *P. likiangensis* and 29 TLP proteins from other plant species (Figure 2). These TLP proteins were divided into three groups. We found that TLPs from gymnosperm species clustered independently into one branch, forming group 2. The TLPs from angiosperm species were clustered into different branches, forming group 1 and group 3. Furthermore, TLPs from monocotyledon species were clustered together, while TLPs from dicotyledon species were clustered into two groups, respectively. The TLPs from the Arecales and Poales species in the monocotyledons were further clustered, respectively. Moreover, the TLPs from the Salicales, Myrtales, and Rosales species in the dicotyledons were also further clustered, respectively.

As expected, *PITLP1* and *PITLP3* were closely related to the TLP proteins from Pinaceae species, and they were clustered into group 2. *PITLP2* was classified into group 1 and had the closest relationship with MrTLP from *Myrica rubra*. In group 3, however, *PITLP4* was clustered with TLP proteins from monocotyledon species.

Tertiary structure analysis plays an important role in revealing the function of proteins. Therefore, the tertiary structure of the four PITLP proteins was homologously modeled to better reveal their functions. So far, the tertiary structure of many thaumatin-like proteins has been resolved. SWISS-MODEL analysis showed that two templates can be used for homology modeling of PITLPs. *PITLP1* and *PITLP3* are similar to the protein structure of Ban-TLP from *Musa acuminata* [39]. *PITLP2* and *PITLP4* are the closest to the protein structure of PaTLP from *Prunus avium* (PDB: 2ahn.1). As shown in Figure 3, the structure of *PITLP1* was the closest to the structure of *PITLP3*, while the structure of *PITLP2* and *PITLP4* had a certain degree of difference, which was in good agreement with the identical result of the amino acid sequence. Importantly, all four PITLP proteins are composed of three domains. Domain I is the N-terminal core functional domain and consists of two antiparallel  $\beta$ -sheets. Domain II is composed of three short  $\alpha$ -helices. Domain III consists of two  $\beta$ -sheets connected by a loop (Figure 3).

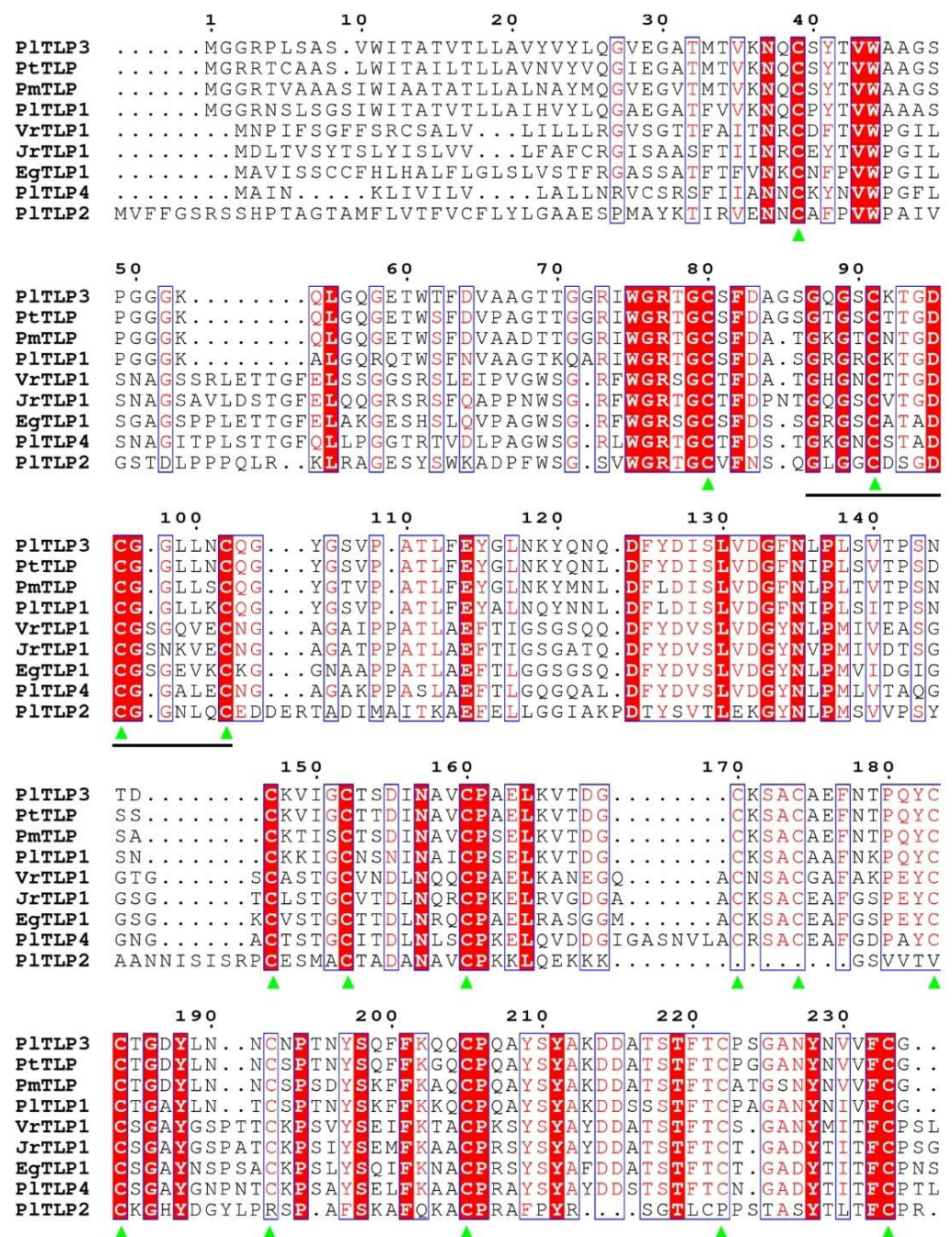


**Figure 1.** Multiple amino acid sequence alignment of PITLPs and five other plant TLPs. These proteins from GenBank are as follows: PtlTLP (*Pinus taeda*, ABQ14359.1), PmtTLP (*Pseudotsuga menziesii*, CAA10492.1), VrtTLP1 (*Vitis riparia*, XP\_034675132.1), TrTLP1 (*Juglans regia*, XP\_018837766.1), and EgTLP1 (*Eucalyptus grandis*, XP\_010029672.2). The 16 conserved cysteine residues are indicated by triangles. The thaumatin family signature (G-x-[GF]-x-C-x-T-[GA]-D-C-x(1,2)-[GQ]-x(2,3)-C) is underlined.



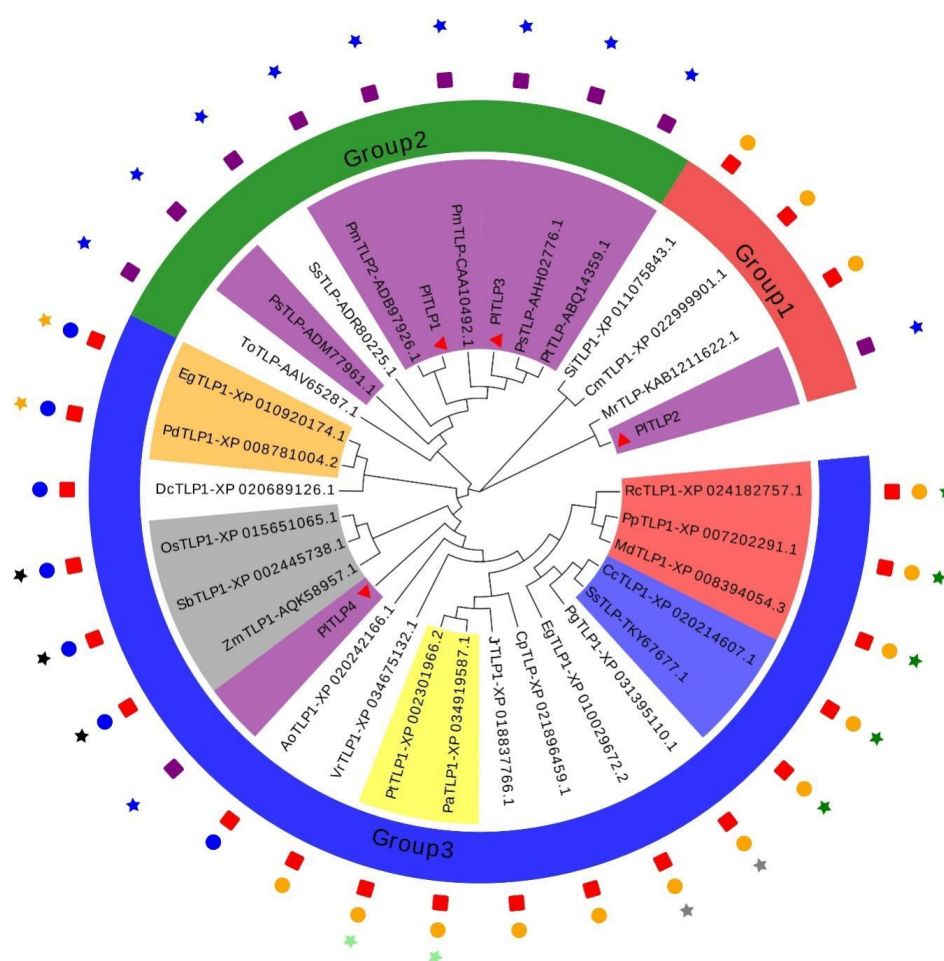


**Figure 2.** Phylogenetic relationships of PITLPs and other known plant TLPs. The tree was constructed by MEGA6.0 using the neighbor-joining method with 1000 bootstrap replicates. Gymnospermae and Angiospermae are indicated with ■ and ■, respectively. Monocotyledons and dicotyledons are indicated with ● and ●, respectively. Coniferales, Arecales, Poales, Salicales, Myrtales, and Rosales were indicated with ★, ★, ★, ★, ★ and ★, respectively. Pinaceae, Palmae, Gramineae, Salicaceae, Leguminosae, and Rosaceae are indicated with purple, orange, gray, yellow, blue, and red backgrounds, respectively.

### 3.2. Expression Profiles of PITLPs

The abundance of *PITLP* transcripts in different tissues of *P. likiangensis* was detected by qPCR. The results showed that the expression of *PITLP1* and *PITLP4* were detected in all tested tissues (Figure 4A). The highest expression levels of *PITLP1*, *PITLP3*, and *PITLP4* were found in young fruits than in other tested tissues, while the highest expression levels of *PITLP2* were found in roots than in other tested tissues. In addition, we found that the relatively lowest expression levels of *PITLP1* and *PITLP4* were found in phloem and twigs, respectively. However, the expression level of *PITLP2* and *PITLP3* were not detected in twigs and roots, respectively.

To confirm whether the *PITLP* genes are involved in pathogen-induced expression, the transcription levels of four *PITLPs* were also detected in needles naturally infected by *L. piceae*. qPCR analysis indicated that the mRNA expression levels of the four *PITLP* genes in the needles of *P. likiangensis* were significantly up-regulated by *L. piceae* (Figure 4B). The highest relative up-regulated expression level induced by *L. piceae* was found in the *PITLP3* gene, which was 9.89-fold higher than the control. In addition, the expression levels of *PITLP1*, *PITLP2*, and *PITLP4* in the infected needles of *P. likiangensis* were 3.18, 1.59, and 2.62-fold higher than those in the control, respectively.

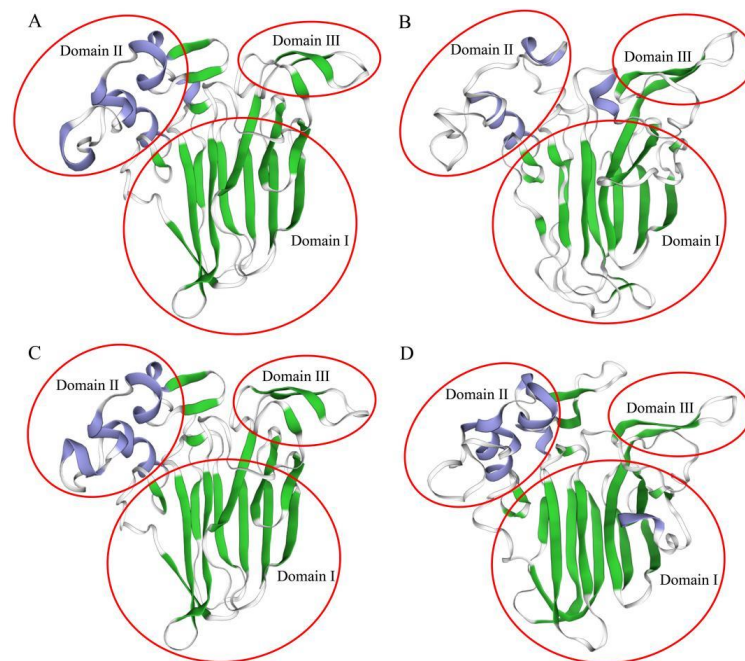


**Figure 3.** Prediction of the tertiary structure of PITLP proteins in *P. likiangensis*. (A) PITLP1; (B) PITLP2; (C) PITLP3; (D) PITLP4.

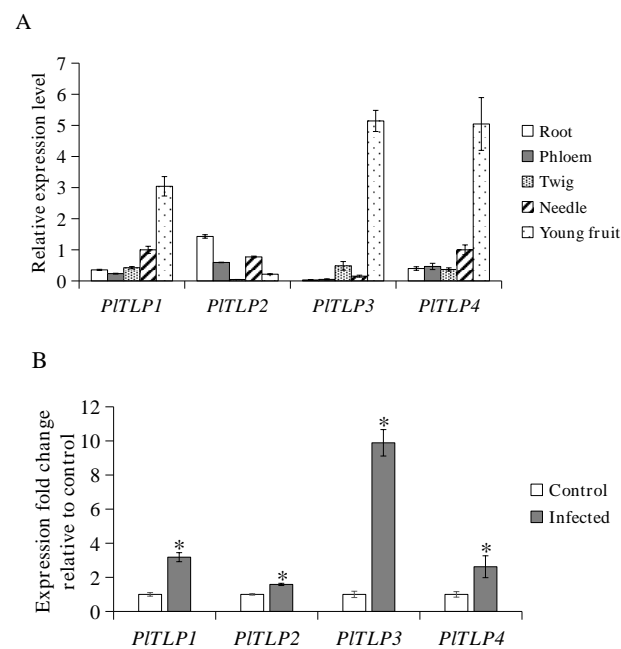


**Figure 4.** Expression profile analysis of PITLPs in *P. likiangensis*. (A) Relative expression of PITLPs in different tissues of *P. likiangensis*. (B) Expression levels of PITLPs in the needles of *P. likiangensis* infected by *L. piceae*. Data represent the mean values  $\pm$  SE ( $n = 3$  biological replicates). Asterisks indicate statistical significance ( $p < 0.05$ , one-way ANOVA).

### 3.3. Expression of Recombinant PITLPs

To study the functions of *P. likiangensis* PITLP proteins, the coding sequences of the four PITLP genes without signal peptides were subcloned into the pET-32a expression vector and then transformed into *E. coli* BL21 (DE3). SDS-PAGE analysis showed that recombinant PITLP1, PITLP2, PITLP3, and PITLP4 were expressed under the induction of IPTG with molecular weights of approximately 39.97, 45.76, 39.85, and 49.57 kDa, respectively, and different concentrations of IPTG had no significant effect on the yield of recombinant PITLP1–4

(Figure S5). In addition, recombinant *PITLP1–4* were mainly formed into insoluble proteins under the induction condition of 37 °C (Figure 5). Optimization of the expression of the recombinant *PITLP1–4* was carried out by lowering the induction temperature. The results showed that the yield of soluble protein in recombinant *PITLP2* and *PITLP4* increased significantly under the induction of low temperature (17 °C) (Figure 5B,D). Moreover, the soluble protein yield of recombinant *PITLP1* and *PITLP3* increased slightly with the decrease in induction temperature (Figure 5A,C). Overall, the optimal conditions for the expression of recombinant *PITLP1–4* were detected to be induced with 0.2 mM IPTG at 17 °C for 3 h. The soluble proteins of recombinant *PITLP1*, *PITLP2*, *PITLP3*, and *PITLP4* were further purified with a Ni-NTA sepharose column, and the concentrations of the purified protein were 0.24 mg/mL, 1.21 mg/mL, 0.2 mg/mL, and 0.92 mg/mL, respectively. The recombinant proteins were diluted to 0.2 mg/mL with ddH<sub>2</sub>O, and 1 nmol of recombinant protein was used for enzymatic analysis and the antifungal activity assay, respectively.

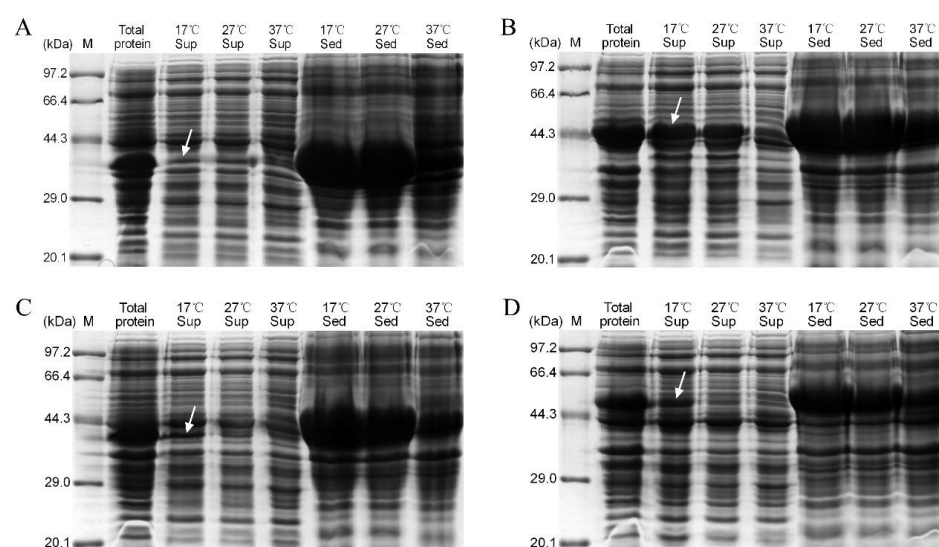


**Figure 5.** SDS-PAGE analysis of recombinant *PITLP* proteins. (A) recombinant *PITLP1*. (B) recombinant *PITLP2*. (C) recombinant *PITLP3*. (D) recombinant *PITLP4*. M: protein marker. Sup: supernatant. Sed: sediment. Arrows indicate the soluble recombinant *PITLPs*.

### 3.4. Characterisation of Enzymatic Activity of Recombinant *PITLPs*

To assess the  $\beta$ -1,3-glucanase activity of recombinant *PITLP1–4*, the enzymatic properties were determined using laminarin as the substrate at different pH and different temperatures. The results showed that the recombinant *PITLP1–4* had  $\beta$ -1,3-glucanase activity (Figure S6). Recombinant *PITLP1–4* exhibited the optimal enzyme activity at pH 4 (6.66, 6.69, 8.11, and 8.89 U/mg, respectively), and maintained relatively high activities in the range of pH 4–8. However, the recombinant *PITLP1–4* had no enzyme activity at pH 3. In addition, the optimal reaction temperature for the enzyme activity of recombinant *PITLP1* was 60 °C, 6.83 U/mg. The enzyme activity of recombinant *PITLP2* gradually increased in the temperature range of 30–80 °C, and 80 °C (7.15 U/mg) was regarded as the optimal reaction temperature for recombinant *PITLP2* in this study. Interestingly, the enzyme activities of recombinant *PITLP3* and *PITLP4* exhibited a similar pattern of increasing first and then decreasing, and the optimal reaction temperature for both of them was 40 °C, with the enzyme activities of 8.11 and 9.93 U/mg, respectively.

### 3.5. Antifungal Activity of Recombinant *PITLPs*

To explore whether *P. likiangensis* *PITLP* had antifungal activity, 1 nmol of (0.2 mg/mL) recombinant *PITLP* protein against *L. piceae*, *F. proliferatum*, *B. cinerea*, and *R. doimaesalongensis* was tested in vitro. The results of the plate test showed that the recombinant *PITLP* proteins exhibited inhibitory effects on all four pathogenic fungi. In addition, we observed that the

recombinant proteins had different degrees of inhibition on fungal growth depending on the plant fungal species (Figure 6). Importantly, the recombinant *PITLP2* had a significant inhibitory effect on *L. piceae*, with a growth inhibition rate of 31.31% compared with the control (Figure 7). The recombinant *PITLP2* and *PITLP3* exhibited significant inhibitory effects on *B. cinerea*, and the inhibitory rates of mycelial growth were 40% and 40.6%, respectively. Recombinant *PITLP3* displayed a 31.03% inhibition rate against *F. proliferatum*. Furthermore, we found that recombinant *PITLP2* still had a 16% inhibition rate on the growth of *R. doimaesalongensis*. Recombinant *PITLP1* and *PITLP4* exhibited the best inhibitory effects on *B. cinerea* compared to the other three tested plant fungi, with inhibition rates of 30.3% and 35.15%, respectively. To determine the 50% inhibition concentration ( $IC_{50}$ ) of antifungal activity against four plant fungal species, 0, 1, 1.5, and 2 nmol of recombinant *PITLP* proteins were used in the assay. However, the results showed that there was no significant difference in the inhibitory effects of the recombinant *PITLP* proteins at different contents on all the tested fungi (data not shown).

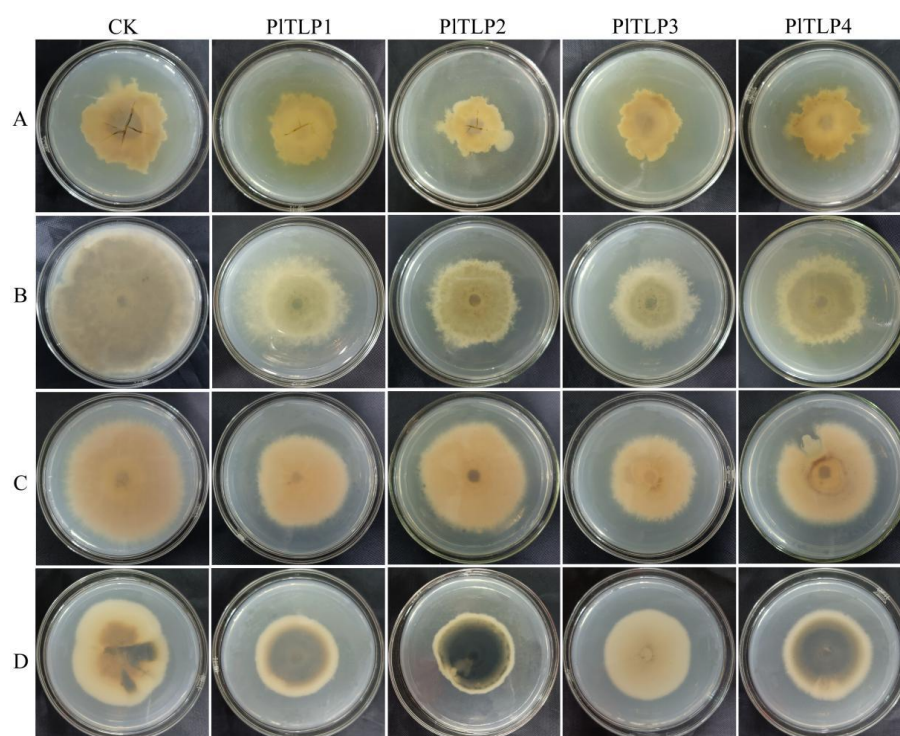


**Figure 6.** Inhibition of fungi growth by recombinant PITLP proteins. (A) *L. piceae*. (B) *B. cinerea*. (C) *F. proliferatum*. (D) *R. doimaesalongensis*. CK: without recombinant PITLP proteins. PITLP1–4: 1 nmol of recombinant protein.

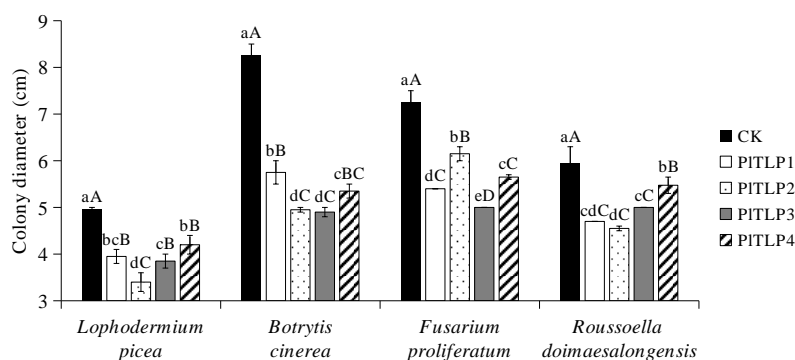


**Figure 7.** Antifungal activity of recombinant PITLP proteins against four plant fungal species. CK: fungi were grown on plates without the recombinant PITLP proteins. PITLP1–4: fungi were grown on



plates containing 1 nmol of recombinant *PITLP1*, *PITLP2*, *PITLP3*, and *PITLP4* proteins, respectively. *L. piceae* were cultured at 25 °C for 15 d; *B. cinerea*, *F. proliferatum*, and *R. doimaesalongensis* were cultured at 25 °C for 5 d. Data represent the mean values  $\pm$  SE ( $n = 3$  independent replicates). Different lowercase letters and uppercase letters indicate statistically significant differences at  $p < 0.05$  and  $p < 0.01$ , respectively.

To investigate the effect of recombinant *PITLP* proteins on mycelial morphology, mycelia of four tested plant fungi were treated with recombinant proteins for 48 h. Microscopic observation revealed that a large number of hyphae of *L. piceae* treated with recombinant *PITLP1–4* proteins were abnormal in morphology, which was not observed in the control treated with ddH<sub>2</sub>O (Figure 8A). Abnormal mycelia were found in the *F. proliferatum* and *R. doimaesalongensis* treated with recombinant *PITLP2* and *PITLP3* proteins, while the hyphae morphology of the *F. proliferatum* and *R. doimaesalongensis* treated with recombinant *PITLP1*, *PITLP4*, and ddH<sub>2</sub>O was normal (Figure 8B,C). In particular, the hyphae morphology of *R. doimaesalongensis* treated with recombinant *PITLP2* had changed, with obvious cell swelling (Figure 8C). In addition, we found that the recombinant *PITLP1–4* proteins had no negative effect on the hyphae of *B. cinerea*.

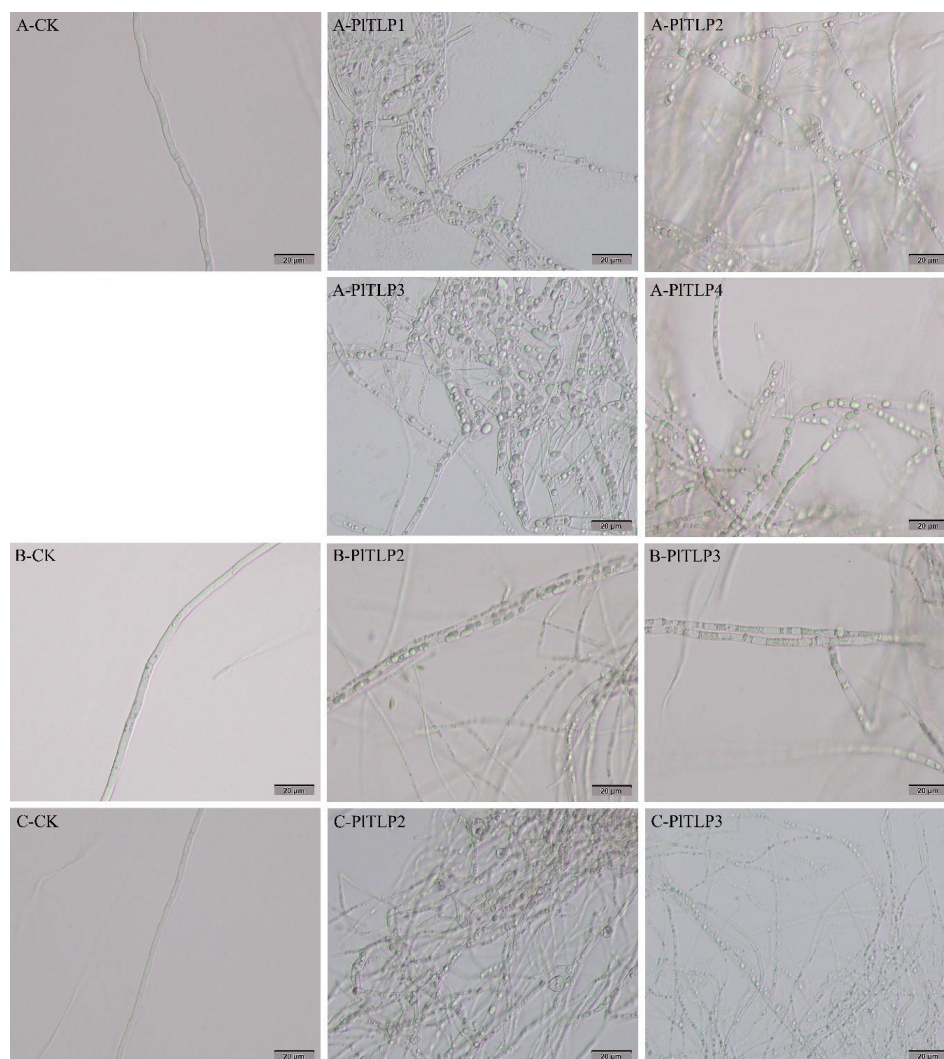


**Figure 8.** Effect of recombinant *PITLP* proteins on fungal hyphae morphology. (A-CK/*PITLP1–4*) *L. piceae*, (B-CK/*PITLP2,3*) *F. proliferatum*, (C-CK/*PITLP2,3*) *R. doimaesalongensis*. CK: The fungal hyphae were treated with ddH<sub>2</sub>O at 25 °C for 48 h. *PITLP1–4*: The fungal hyphae were treated with

1 nmol of recombinant PITLP1, PITLP2, PITLP3, and PITLP4, respectively, at 25 °C for 48 h. Each fungal species was performed in three independent replicates.

#### 4. Discussion

In recent years, a large number of genes encoding TLP proteins have been identified in fungi, animals, and plants [12]. TLP genes in plants have been found to be involved in plant defense responses and other developmental processes [17,40]. In this study, we isolated and characterized four TLP genes (*PITLP1–PITLP4*) from *P. likiangensis*. Previous studies have shown that most TLP proteins have N-signal peptide sequences and are localized in extracellular or intracellular [11,41]. The prediction of signal peptide and subcellular localization indicated that all *PITLP* proteins were extracellularly secreted proteins. Generally, TLPs contain the thaumatin family signature sequence G-x-[GF]-x-C-x-T-[GA]-D-C-x(1,2)-[GQ]-x(2,3)-C, and are rich in cysteine residues [42]. Among the four *PITLPs* in *P. likiangensis*, *PITLP1*, *PITLP3*, and *PITLP4*, all have a typical thaumatin family signature and contain 16 cysteine residues. However, PROSITE prediction indicated that *PITLP2* does not have the signature sequence of the thaumatin family and only contains 10 cysteine residues. The thaumatin-like protein (TaPR5) from wheat has also been reported to contain 10 conserved cysteine residues [43]. In addition, small TLPs of approximately 16–17 kDa, mainly from conifers and cereals, were found to contain 10 cysteine residues at conserved positions [42,44]. In the phylogenetic tree, *PITLPs* are closely related to TLPs with antifungal or glucanase activities, suggesting that *PITLPs* may have similar functions. All *PITLPs* were structurally similar to the antifungal Permatin of *Avena nuda* [18], further suggesting that *PITLPs* may have antifungal activity.

Many studies have found that plant TLP is a family encoded by multiple genes, such as in *P. monticola* [22], *P. notoginseng* [11], and *V. vinifera* [12]. Distribution of TLP transcripts in unique tissues suggests that it may be a potential component of the plant innate immune system. We found that the expression of *PITLP1* and *PITLP3* genes was detected in all the tested tissues. The highest expression levels of *PITLP1*, *PITLP3*, and *PITLP4* were found in the young fruits of *P. likiangensis*, while the highest expression levels of *PITLP2* were found in the roots of *P. likiangensis*. These results suggest that most of the *PITLP* genes may be required in the fruits development of *P. likiangensis*. A previous study indicated that the expression of the *CITLP27* gene was detected in multiple organs of watermelon, and the highest expression level was in the root [6]. In addition, a TLP gene from cherry (*Prunus avium*) was reported to have the highest mRNA expression level in mature fruits [45]. The expression of the *PepTLP* gene in *Capsicum annuum* is developmentally regulated during its fruit ripening [46]. Importantly, studies have proved that plant TLP genes are involved in the defense response to pathogen infection, and multiple TLP genes in plants can simultaneously respond to one or several pathogen infections. For example, mRNA expression levels of three TLP genes from *Polyporus umbellatus* were significantly increased during *Armillaria mellea* invasion [41]. Four TLP genes have been proven to be involved in the defense responses of *P. notoginseng* to *A. panax* infection [11]. In addition, it has been reported that the expression levels of six TLP genes in grapes were simultaneously up-regulated after inoculation with three pathogenic fungi (*Elsinoe ampelina*, *Erysiphe necator*, and *B. cinerea*) [12]. In our study, the expression levels of four TLP genes (especially *PITLP3*) were significantly up-regulated during the natural invasion of *P. likiangensis* needles by *L. piceae*. The results suggest that multiple *PITLP* genes may be simultaneously involved in the defense response of *P. likiangensis* to *L. piceae*.

The prokaryotic expression system provides an effective and feasible pathway for the study of gene function [47]. In this work, four *PITLP* genes were successfully expressed in *E. coli* BL21(DE3) using the pET-32a vector, and the molecular weights of recombinant PITLP proteins were in the range of 39.85–49.57 kDa, which was similar to that of the recombinant PnTLP2 protein (45 kDa) of *P. notoginseng* expressed by the pET-32a vector [11]. In addition, the molecular weight of the recombinant *PITLP* proteins was larger than that of the reported recombinant TLP protein (24.6 kDa) of *P. sylvestris* [17], and the reported

recombinant His-CITLP27 protein (26.9 kDa) of watermelon [6], but smaller than that of the reported recombinant Nus-Permatin protein (83 kDa) of naked oat [18]. The significant difference in their molecular weight was mainly caused by the different expression vectors. SDS-PAGE analysis showed that IPTG treatment at different concentrations had no significant effect on the production of the four recombinant PITLP proteins, which was similar to that reported by Snepste et al. [17]. Many studies have shown that temperature plays an important role in improving the soluble distribution of recombinant proteins [47,48]. Our study found that lowering the induction temperature significantly increased the soluble protein yield of recombinant *PITLP2* and *PITLP4*, and slightly increased the soluble protein yield of recombinant *PITLP1* and *PITLP3*. In future work, to further improve the solubility of recombinant *PITLP1* and *PITLP3*, we believe that the use of different fusion tags will be a good attempt [47].

$\beta$ -1,3-glucanase plays an important role in the destruction of the fungal cell wall or membrane [49]. Some plant TLPs have been found to have  $\beta$ -1,3-glucanase activity in vitro. It has been reported that both Pru-TLP from cherry and Mal-TLP from apple exhibit a reasonably high endo- $\beta$ -1,3-glucanase activity [29]. TLP proteins extracted from the leaves of multiple transgenic rice plants have been shown to possess a wide range of  $\beta$ -1,3-glucanase activities [32]. In this work, four recombinant *PITLPs* were found to have  $\beta$ -1,3-glucanase activity, and the optimal reaction pH of these recombinant *PITLPs* was determined to be 4. A previous study showed that the optimum pH for Ban-TLP enzyme activity in banana was also determined to be 4, but it only had a weak endo- $\beta$ -1,3-glucanase activity [50]. Two TLP proteins from peach were reported to have higher  $\beta$ -1,3-glucanase activity at pH 6 than at other pHs [51]. In addition, we found that recombinant *PITLPs* maintained a relatively high enzyme activity in the temperature range of 30–60 °C. To our knowledge, this is the first report of TLP proteins with  $\beta$ -1,3-glucanase activity from coniferous species.

Most TLP proteins have a broad spectrum of antifungal activity in vitro. For example, the recombinant ObTLP1 obtained by prokaryotic expression exhibited an inhibitory effect on the mycelial growth of two phytopathogenic fungi (*S. sclerotiorum* and *B. cinerea*) [52]. In vitro antifungal activity assay indicated that the recombinant AdTLP significantly inhibited the spore germination of three fungal species (*F. oxysporum*, *Fusarium solani*, and *B. cinerea*), and exhibited an inhibitory effect on the hyphae growth of *Rhizoctonia solani* [53]. Moreover, recombinant His-CITLP27 exhibited significant antifungal activity against the growth of five fungal species, including *Fusarium oxysporum* f.sp. *niveum* race 1, *Fusarium solani* f.sp. *cucurbitae* race 1, *Fusarium oxysporum* f.sp. *melonis*, *Fusarium verticillioides*, and *Didymella bryoniae* [6]. The plate assay showed that the four recombinant *PITLP* proteins had significant antifungal activities against four tested plant fungi. Among them, recombinant *PITLP2* has the best inhibition effect on the mycelial growth of *L. piceae* and *R. doimaesalongensis*, and recombinant *PITLP3* has the best inhibition effect on the mycelial growth of *B. cinerea* and *F. proliferatum*. Our results have shown that almost all of the plant TLP proteins with antifungal activity had obvious inhibitory effects on *Fusarium* species and *B. cinerea*.

Furthermore, we also observed the effect of recombinant *PITLP* proteins on the morphology of hyphae of the four tested fungi. Microscopic observation revealed that the four recombinant *PITLP* proteins had an obvious negative effect on the morphology of *L. piceae* hyphae (Figure 8). The same morphological changes were also observed in *F. proliferatum* and *R. doimaesalongensis* treated with recombinant *PITLP2* and *PITLP3*. In addition, similar morphological changes were found in the hyphae of *F. oxysporum* treated with recombinant Nus-permatin reported by Liu et al. [18], and they found that this change was due to the penetration of fungal cell membrane and the production of ROS in cells caused by TLP protein. Interestingly, we found that recombinant *PITLP2* also caused cell swelling in *R. doimaesalongensis* (Figure 8C). It has been reported that recombinant AdTLP of *Arachis diogeni* induces the hyperbranched morphological changes in the mycelium of

*B. cinerea* [53]. However, in our study, none of the four recombinant *PITLP* proteins caused changes in mycelial morphology of *B. cinerea*.

## 5. Conclusions

In this study, four members of the PR5 family were successfully isolated and identified from *P. likiangensis*. qPCR analysis showed that the expression levels of four *PITLP* genes were significantly up-regulated by *L. piceae* invasion. These four genes were successfully expressed in *E. coli* by a prokaryotic expression system, and further exploration is needed for the mass production of soluble proteins of recombinant *PITLP1* and *PITLP3*. Interestingly, four recombinant *PITLP* proteins exhibited significant  $\beta$ -1,3-glucanase activity. The in vitro antifungal activity assay showed that the recombinant *PITLP* proteins could significantly inhibit the mycelial growth of four tested plant pathogenic fungi, including *L. piceae*, and induce the morphological changes of the mycelia of *L. piceae*, *F. proliferatum*, and *R. doimaesalongensis*. These results provide support for the important role of *PITLP* genes in the defense of *P. likiangensis* against *L. piceae* and enrich the biological control materials for plant pathogenic fungi.

**Supplementary Materials:** The following are available online at <https://www.mdpi.com/article/10.3390/f12091268/s1>, Figure S1. Nucleotide sequence and the deduced amino acid sequence of the *PITLP1* gene. The start codon is shown by bold font. The stop codon is indicated by an asterisk. The signal peptide sequences are underlined. The thaumatin family signature (G-x-[GF]-x-C-x-T-[GA]-D-C-x(1,2)-[GQ]-x(2,3)-C) is shaded in gray. Figure S2. Nucleotide sequence and the deduced amino acid sequence of the *PITLP2* gene. The start codon is shown by bold font. The stop codon is indicated by an asterisk. The signal peptide sequences are underlined. Figure S3. Nucleotide sequence and the deduced amino acid sequence of the *PITLP3* gene. The start codon is shown by bold font. The stop codon is indicated by an asterisk. The signal peptide sequences are underlined. The thaumatin family signature (G-x-[GF]-x-C-x-T-[GA]-D-C-x(1,2)-[GQ]-x(2,3)-C) is shaded in gray. Figure S4. Nucleotide sequence and the deduced amino acid sequence of the *PITLP4* gene. The start codon is shown by bold font. The stop codon is indicated by an asterisk. The signal peptide sequences are underlined. The thaumatin family signature (G-x-[GF]-x-C-x-T-[GA]-D-C-x(1,2)-[GQ]-x(2,3)-C) is shaded in gray. Figure S5. SDS-PAGE analysis of recombinant *PITLP* proteins induced with different concentrations of IPTG (0, 0.2, 0.4, 0.6, 0.8 and 1.0 mM). A: recombinant *PITLP1*. B: recombinant *PITLP2*. C: recombinant *PITLP3*. D: recombinant *PITLP4*. M: protein marker. CK: pET-32a in *E. coli* BL21(DE3). Arrows indicate the recombinant *PITLP* proteins. Figure S6. Effects of pH and temperature on the  $\beta$ -1,3-glucanase activity of recombinant *PITLP1*–4. Determination of the optimal pH was measured in 50 mM sodium acetate (pH 3–6) and Tris-HCl (pH 7–9), at 40 °C for 30 min. Determination of the optimal temperature was measured in 50 mM sodium acetate (pH 6), at 30–80 °C for 30 min. Data represent mean values  $\pm$  SE (n = 3 technical replicates). Table S1. Primers for PCR and qPCR.

**Author Contributions:** Y.L. (Yufeng Liu) conceived, designed, and performed the experiments, analyzed the data, and wrote the manuscript; L.L. analyzed the data; L.L., S.Y. and Q.Z. collected plant samples; S.H., C.Y. and Y.L. (Yinggao Liu) supervised the project; F.O.A. and Y.L. (Yinggao Liu) reviewed the manuscript. All authors have read and agreed to the published version of the manuscript.

**Funding:** This research received no external funding.

**Acknowledgments:** We would like to thank Luding forest farm for their help in sample collection.

**Conflicts of Interest:** The authors declare no conflict of interests.

## References

1. Kazan, K.; Lyons, R. Intervention of Phytohormone Pathways by Pathogen Effectors. *Plant Cell* **2014**, *26*, 2285–2309. [CrossRef]
2. Bonello, P.; Gordon, T.R.; Herms, D.A.; Wood, D.L.; Erbilen, N. Nature and ecological implications of pathogen-induced systemic resistance in conifers: A novel hypothesis. *Physiol. Mol. Plant Pathol.* **2006**, *68*, 95–104. [CrossRef]
3. Cao, J.; Lv, Y.Q.; Hou, Z.R.; Li, X.; Ding, L.N. Expansion and evolution of thaumatin-like protein (TLP) gene family in six plants. *Plant Growth Regul.* **2016**, *79*, 299–307. [CrossRef]



4. Hakim, Ullah, A.; Hussain, A.; Shaban, M.; Khan, A.H.; Alariqi, M.; Gul, S.; Jun, Z.; Lin, S.; Li, J.Y.; et al. Osmotin: A plant defense tool against biotic and abiotic stresses. *Plant Physiol. Biochem.* **2018**, *123*, 149–159. [\[CrossRef\]](#)
5. Musidlak, O.; Nawrot, R.; Goździcka-Józefiak, A. Which Plant Proteins Are Involved in Antiviral Defense? Review on In Vivo and In Vitro Activities of Selected Plant Proteins against Viruses. *Int. J. Mol. Sci.* **2017**, *18*, 2300. [\[CrossRef\]](#)
6. Zhang, M.; Xu, J.H.; Liu, G.; Yang, X.P. Antifungal properties of a thaumatin-like protein from watermelon. *Acta. Physiol. Plant* **2018**, *40*, 186. [\[CrossRef\]](#)
7. Kovalchuk, A.; Keriö, S.; Oghenekaro, A.O.; Jaber, E.; Raffaello, T.; Asiegbu, F.O. Antimicrobial Defenses and Resistance in Forest Trees: Challenges and Perspectives in a Genomic Era. *Annu. Rev. Phytopathol.* **2013**, *51*, 221–244. [\[CrossRef\]](#)
8. Petre, B.; Major, I.; Rouhier, N.; Duplessis, S. Genome-wide analysis of eukaryote thaumatin-like proteins (TLPs) with an emphasis on poplar. *BMC Plant Biol.* **2011**, *11*, 33. [\[CrossRef\]](#)
9. Meng, F.L.; Wang, J.; Wang, X.; Li, Y.X.; Zhang, X.Y. Expression analysis of thaumatin-like proteins from *Bursaphelenchus xylophilus* and *Pinus massoniana*. *Physiol. Mol. Plant Pathol.* **2017**, *100*, 178–184. [\[CrossRef\]](#)
10. Franco, S.D.F.; Baroni, R.M.; Carazzolle, M.F.; Teixeira, P.J.P.L.; Reis, O.; Pereira, G.A.G.; Mondego, J.M.C. Genomic analyses and expression evaluation of thaumatin-like gene family in the cacao fungal pathogen *Moniliophthora perniciosa*. *Biochem. Biophys. Res. Commun.* **2015**, *466*, 629–636. [\[CrossRef\]](#)
11. Li, X.; Li, S.; Qiu, B.L.; Zhang, Y.P.; Cui, X.M.; Ge, F.; Liu, D.Q. Thaumatin-like protein genes of *Panax notoginseng* confers resistance to *Alternaria panax*. *Physiol. Mol. Plant Pathol.* **2020**, *112*, 101537. [\[CrossRef\]](#)
12. Yan, X.X.; Qiao, H.B.; Zhang, X.M.; Guo, C.L.; Wang, M.N.; Wang, Y.J.; Wang, X.P. Analysis of the grape (*Vitis vinifera* L.) thaumatin-like protein (TLP) gene family and demonstration that TLP29 contributes to disease resistance. *Sci. Rep.* **2017**, *7*, 4269. [\[CrossRef\]](#) [\[PubMed\]](#)
13. Smole, U.; Bublin, M.; Radauer, C.; Ebner, C.; Breiteneder, H. Mal d 2, the Thaumatin-Like Allergen from Apple, Is Highly Resistant to Gastrointestinal Digestion and Thermal Processing. *Int. Arch. Allergy Immunol.* **2008**, *147*, 289–298. [\[CrossRef\]](#)
14. Guo, J.; Zhao, X.; Wang, H.L.; Yu, T.; Miao, Y.; Zheng, X.D. Expression of the LePR5 gene from cherry tomato fruit induced by *Cryptococcus laurentii* and the analysis of LePR5 protein antifungal activity. *Postharvest Biol. Technol.* **2016**, *111*, 337–344. [\[CrossRef\]](#)
15. Rather, I.A.; Awasthi, P.; Mahajan, V.; Bedi, Y.S.; Vishwakarma, R.A.; Gandhi, S.G. Molecular cloning and functional characterization of an antifungal PR-5 protein from *Ocimum basilicum*. *Gene* **2015**, *558*, 143–151. [\[CrossRef\]](#) [\[PubMed\]](#)
16. Hayashi, M.; Shiro, S.; Kanamori, H.; Mori-Hosokawa, S.; Sasaki-Yamagata, H.; Sayama, T.; Nishioka, M.; Takahashi, M.; Ishimoto, M.; Katayose, Y.; et al. A Thaumatin-Like Protein, Rj4, Controls Nodule Symbiotic Specificity in Soybean. *Plant Cell Physiol.* **2014**, *55*, 1679–1689. [\[CrossRef\]](#) [\[PubMed\]](#)
17. Šnepšte, I.; Škipars, V.; Krivmane, B.; Brūna, L.; Ruņģis, D. Characterization of a *Pinus sylvestris* thaumatin-like protein gene and determination of antimicrobial activity of the in vitro expressed protein. *Tree Genet. Genomes* **2018**, *14*, 58. [\[CrossRef\]](#)
18. Liu, J.; Han, D.P.; Shi, Y.W. Gene Cloning, Expression, and Antifungal Activities of Permatin from Naked Oat (*Avena nuda*). *Probiotics Antimicrob. Proteins* **2019**, *11*, 299–309. [\[CrossRef\]](#)
19. Rout, E.; Nanda, S.; Joshi, R.K. Molecular characterization and heterologous expression of a pathogen induced PR5 gene from garlic (*Allium sativum* L.) conferring enhanced resistance to necrotrophic fungi. *Eur. J. Plant Pathol.* **2016**, *144*, 345–360. [\[CrossRef\]](#)
20. Mahdavi, F.; Sariah, M.; Maziah, M. Expression of Rice Thaumatin-Like Protein Gene in Transgenic Banana Plants Enhances Resistance to Fusarium Wilt. *Appl. Biochem. Biotechnol.* **2012**, *166*, 1008–1019. [\[CrossRef\]](#)
21. Munis, M.F.H.; Tu, L.; Deng, F.L.; Tan, J.F.; Xu, L.; Xu, S.C.; Long, L.; Zhang, X.L. A thaumatin-like protein gene involved in cotton fiber secondary cell wall development enhances resistance against *Verticillium dahliae* and other stresses in transgenic tobacco. *Biochem. Biophys. Res. Commun.* **2010**, *393*, 38–44. [\[CrossRef\]](#)
22. Liu, J.J.; Zamani, A.; Ekramoddoullah, A.K.M. Expression profiling of a complex thaumatin-like protein family in western white pine. *Planta* **2010**, *231*, 637–651. [\[CrossRef\]](#)
23. Sun, W.B.; Zhou, Y.; Movahedi, A.; Wei, H.; Zhuge, Q. Thaumatin-like protein (Pe-TLP) acts as a positive factor in transgenic poplars enhanced resistance to spots disease. *Physiol. Mol. Plant Pathol.* **2020**, *112*, 101512. [\[CrossRef\]](#)
24. Muoki, R.C.; Paul, A.; Kaachra, A.; Kumar, S. Membrane localized thaumatin-like protein from tea (*CsTLP*) enhanced seed yield and the plant survival under drought stress in *Arabidopsis thaliana*. *Plant Physiol. Biochem.* **2021**, *163*, 36–44. [\[CrossRef\]](#) [\[PubMed\]](#)
25. Li, Z.S.; Wang, X.Y.; Cui, Y.P.; Qiao, K.K.; Zhu, L.F.; Fan, S.L.; Ma, Q.F. Comprehensive Genome-Wide Analysis of Thaumatin-Like Gene Family in Four Cotton Species and Functional Identification of *GhTLP19* Involved in Regulating Tolerance to *Verticillium dahlia* and Drought. *Front. Plant Sci.* **2020**, *11*, 575015. [\[CrossRef\]](#) [\[PubMed\]](#)
26. Van der Maelen, E.; Rezaei, M.N.; Struyf, N.; Proost, P.; Verstrepen, K.J.; Courtin, C.M. Identification of a Wheat Thaumatin-like Protein That Inhibits *Saccharomyces cerevisiae*. *J. Agric. Food Chem.* **2019**, *67*, 10423–10431. [\[CrossRef\]](#)
27. Wang, L.; Yang, L.; Zhang, J.; Dong, J.; Yu, J.; Zhou, J.; Zhuge, Q. Cloning and characterization of a thaumatin-like protein gene *PeTLP* in *Populus deltoides* × *P. euramericana* cv. ‘Nanlin895’. *Acta. Physiol. Plant* **2013**, *35*, 2985–2998. [\[CrossRef\]](#)
28. Osmond, R.I.W.; Hrmova, M.; Fontaine, F.; Imberty, A.; Fincher, G.B. Binding interactions between barley thaumatin-like proteins and (1,3)- $\beta$ -D-glucans. *Eur. J. Biochem.* **2001**, *268*, 4190–4199. [\[CrossRef\]](#)
29. Menu-Bouaouiche, L.; Vriet, C.; Peumans, W.J.; Barre, A.; Van Damme, E.J.M.; Rougé, P. A molecular basis for the endo- $\beta$ 1,3-glucanase activity of the thaumatin-like proteins from edible fruits. *Biochimie* **2003**, *85*, 123–131. [\[CrossRef\]](#)
30. Theis, T.; Stahl, U. Antifungal proteins: Targets, mechanisms and prospective applications. *Cell. Mol. Life Sci.* **2004**, *61*, 437–455. [\[CrossRef\]](#)

31. Grenier, J.; Potvin, C.; Trudel, J.; Asselin, A. Some thaumatin-like proteins hydrolyse polymeric  $\beta$ -1,3-glucans. *Plant J.* **1999**, *19*, 473–480. [\[CrossRef\]](#)
32. Aghazadeh, R.; Zamani, M.; Motallebi, M.; Moradyar, M. Agrobacterium-Mediated Transformation of the *Oryza sativa* Thaumatin-Like Protein to Canola (R Line Hyola308) for Enhancing Resistance to *Sclerotinia sclerotiorum*. *Iran. J. Biotechnol.* **2017**, *15*, 201–207. [\[CrossRef\]](#)
33. de Freitas, C.D.T.; Lopes, J.L.D.S.; Beltramini, L.M.; de Oliveira, R.S.B.; Oliveira, J.T.A.; Ramos, M.V. Osmotin from *Calotropis procera* latex: New insights into structure and antifungal properties. *Biochim. Biophys. Acta (BBA)—Biomembr.* **2011**, *1808*, 2501–2507. [\[CrossRef\]](#) [\[PubMed\]](#)
34. Tanney, J.B.; Seifert, K.A. *Lophodermium resinosum* sp. nov. from red pine (*Pinus resinosa*) in Eastern Canada. *Botany* **2017**, *95*, 773–784. [\[CrossRef\]](#)
35. Korkama-Rajala, T.; Müller, M.M.; Pennanen, T. Decomposition and Fungi of Needle Litter from Slow- and Fast-growing Norway Spruce (*Picea abies*) Clones. *Microb. Ecol.* **2008**, *56*, 76–89. [\[CrossRef\]](#)
36. Liu, Y.F.; Liu, L.J.; Yang, S.; Zeng, Q.; He, Z.R.; Liu, Y.G. Cloning, Characterization and Expression of the Phenylalanine Ammonia-Lyase Gene (*PaPAL*) from Spruce *Picea asperata*. *Forests* **2019**, *10*, 613. [\[CrossRef\]](#)
37. Tamura, K.; Stecher, G.; Peterson, D.; Filipski, A.; Kumar, S. MEGA6: Molecular evolutionary genetics analysis version 6.0. *Mol. Biol. Evol.* **2013**, *30*, 2725–2729. [\[CrossRef\]](#) [\[PubMed\]](#)
38. Livak, K.J.; Schmittgen, T.D. Analysis of relative gene expression data using real-time quantitative PCR and the  $2^{-\Delta\Delta CT}$  method. *Methods* **2001**, *25*, 402–408. [\[CrossRef\]](#)
39. Leone, P.; Menu-Bouaouiche, L.; Peumans, W.J.; Payan, F.; Barre, A.; Roussel, A.; Van Damme, E.J.M.; Rougé, P. Resolution of the structure of the allergenic and antifungal banana fruit thaumatin-like protein at 1.7-Å. *Biochimie* **2006**, *88*, 45–52. [\[CrossRef\]](#)
40. Monteiro, S.; Barakat, M.; Piçarra-Pereira, M.A.; Teixeira, A.R.; Ferreira, R.B. Osmotin and Thaumatin from Grape: A Putative General Defense Mechanism Against Pathogenic Fungi. *Phytopathology* **2003**, *93*, 1505–1512. [\[CrossRef\]](#)
41. Liu, M.; Zhang, D.; Xing, Y.; Guo, S. Cloning and expression of three thaumatin-like protein genes from *Polyporus umbellatus*. *Acta Pharm. Sin. B* **2017**, *7*, 373–380. [\[CrossRef\]](#)
42. Liu, J.J.; Sturrock, R.; Ekramoddoullah, A.K.M. The superfamily of thaumatin-like proteins: Its origin, evolution, and expression towards biological function. *Plant Cell Rep.* **2010**, *29*, 419–436. [\[CrossRef\]](#)
43. Wang, X.; Tang, C.; Deng, L.; Cai, G.; Liu, X.; Liu, B.; Han, Q.; Buchenauer, H.; Wei, G.; Han, D.; et al. Characterization of a pathogenesis-related thaumatin-like protein gene *TaPR5* from wheat induced by stripe rust fungus. *Physiol. Plant* **2010**, *139*, 27–38. [\[CrossRef\]](#)
44. O’Leary, S.J.B.; Poullis, B.A.D.; von Aderkas, P. Identification of two thaumatin-like proteins (TLPs) in the pollination drop of hybrid yew that may play a role in pathogen defence during pollen collection. *Tree Physiol.* **2007**, *27*, 1649–1659. [\[CrossRef\]](#)
45. Fils-Lycaon, B.R.; Wiersma, P.A.; Eastwell, K.C.; Sautiere, P. A Cherry Protein and Its Gene, Abundantly Expressed in Ripening Fruit, Have Been Identified as Thaumatin-Like. *Plant Physiol.* **1996**, *111*, 269–273. [\[CrossRef\]](#)
46. Kim, Y.S.; Park, J.Y.; Kim, K.S.; Ko, M.K.; Cheong, S.J.; Oh, B. A thaumatin-like gene in nonclimacteric pepper fruits used as molecular marker in probing disease resistance, ripening, and sugar accumulation. *Plant Mol. Biol.* **2002**, *49*, 125–135. [\[CrossRef\]](#)
47. Esposito, D.; Chatterjee, D.K. Enhancement of soluble protein expression through the use of fusion tags. *Curr. Opin. Biotechnol.* **2006**, *17*, 353–358. [\[CrossRef\]](#)
48. Urban, A.; Ansmant, I.; Motorin, Y. Optimisation of expression and purification of the recombinant Yol066 (Rib2) protein from *Saccharomyces cerevisiae*. *J. Chromatogr. B* **2003**, *786*, 187–195. [\[CrossRef\]](#)
49. Wawra, S.; Fesel, P.; Widmer, H.; Timm, M.; Seibel, J.; Leson, L.; Kessler, L.; Nostadt, R.; Hilbert, M.; Langen, G. The fungal-specific  $\beta$ -glucan-binding lectin FGB1 alters cell-wall composition and suppresses glucan-triggered immunity in plants. *Nat. Commun.* **2016**, *7*, 13188. [\[CrossRef\]](#)
50. Barre, A.; Peumans, W.J.; Menu-Bouaouiche, L.; Van Damme, E.J.M.; May, G.D.; Fernandez Herrera, A.; Van Leuven, F.; Rougé, P. Purification and structural analysis of an abundant thaumatin-like protein from ripe banana fruit. *Planta* **2000**, *211*, 791–799. [\[CrossRef\]](#)
51. Palacín, A.; Tordesillas, L.; Gamboa, P.; Sanchez-Monge, R.; Cuesta-Herranz, J.; Sanz, M.L.; Barber, D.; Salcedo, G.; Díaz-Perales, A. Characterization of peach thaumatin-like proteins and their identification as major peach allergens. *Clin. Exp. Allergy* **2010**, *40*, 1422–1430. [\[CrossRef\]](#) [\[PubMed\]](#)
52. Misra, R.C.; Sandeep; Kamthan, M.; Kumar, S.; Ghosh, S. A thaumatin-like protein of *Ocimum basilicum* confers tolerance to fungal pathogen and abiotic stress in transgenic Arabidopsis. *Sci. Rep.* **2016**, *6*, 25340. [\[CrossRef\]](#)
53. Singh, N.K.; Kumar, K.R.R.; Kumar, D.; Shukla, P.; Kirti, P.B. Characterization of a Pathogen Induced Thaumatin-Like Protein Gene *AdTLP* from *Arachis diogeni*, a Wild Peanut. *PLoS ONE* **2013**, *8*, e83963.